AIP | Applied Physics Letters

Polymeric distributed feedback lasers by room-temperature nanoimprint lithography

Elisa Mele, Andrea Camposeo, Ripalta Stabile, Pompilio Del Carro, Francesca Di Benedetto, Luana Persano, Roberto Cingolani, and Dario Pisignano

Citation: Applied Physics Letters **89**, 131109 (2006); doi: 10.1063/1.2357116
View online: http://dx.doi.org/10.1063/1.2357116
View Table of Contents: http://scitation.aip.org/content/aip/journal/apl/89/13?ver=pdfcov
Published by the AIP Publishing

APPLIED PHYSICS LETTERS **89**, 131109 (2006)

Polymeric distributed feedback lasers by room-temperature nanoimprint lithography

Elisa Mele,[a] Andrea Camposeo, Ripalta Stabile, Pompilio Del Carro,
Francesca Di Benedetto, Luana Persano, Roberto Cingolani, and Dario Pisignano
National Nanotechnology Laboratory (NNL) of CNR-INFM, Università degli Studi di Lecce,
c/o Distretto Tecnologico ISUFI, via Arnesano, I-73100 Lecce, Italy

(Received 20 April 2006; accepted 3 August 2006; published online 27 September 2006)

Room temperature nanoimprinting lithography is used to realize a distributed feedback laser by direct dry pressing of the conjugated polymer (poly[2-methoxy-5-(2-ethylhexyloxy)-1,4-phenylenevinylene]). The laser device exhibits emission at 630 nm with a pump threshold of 25 μJ/cm^2 and a polarization contrast of the emitted light as large as 0.91. Therefore, room temperature nanoimprint lithography turns out to be very effective for producing stable patterns on light-emitting polymers for the one-step fabrication of nanopatterned optoelectronic devices. © *2006 American Institute of Physics*. [DOI: 10.1063/1.2357116]

Semiconducting conjugated polymers are attractive materials for applications in optoelectronic devices, including polymer light-emitting diodes,[1] photodetectors,[2] photovoltaic cells,[3] full-color displays,[4] and field-effect transistors.[5] In addition, they present interesting characteristics for solid-state lasers[6] by virtue of their high photoluminescence efficiency, large cross section for stimulated emission, and optical gain under low injection rate over the whole visible spectrum. An important requirement to achieve lasing action is the optical feedback in the device. Among a variety of resonator geometries,[7–9] the use of a structured medium providing distributed feedback (DFB) along the direction of propagation by a periodic modulation of refractive index or gain is particularly effective.[10] Nowadays, different approaches have been developed to realize organic DFB structures, involving both standard and soft lithographic techniques,[11–14] and nanoimprinting methods.[15,16]

Nanoimprint lithography[15] (NIL) is a high throughput technique based on the deformation of a thermoplastic film under the concomitant application of pressure (about 100 Pa) and high temperature (up to 250 °C). In the conventional NIL, a rigid nanostructured template is pressed onto the film and heated above its glass transition temperature (T_g). Upon heating, the polymer becomes fluid and fills the recessed spaces of the stamp, forming the pattern. Then, the system is cooled below T_g and the mold is removed. Such temperature cycle strongly limits the application of NIL for directly structuring organic conjugated molecules in air, as the optoelectronic properties of the active material undergo irreversible degradation due to oxygen diffusion and incorporation into the molecular backbones.[17] Therefore, patterning light-emitting molecules generally needs controlled atmosphere,[18] with a consequent increase of the complexity of the experimental setup and of the overall cost of the lithography.

Recently, we developed the NIL at room temperature (RT-NIL, first applied on lithographic resists)[19] on active organics, which allowed us to retain the light-emitting performances of molecules. Initially ideated for nonthermoplastic oligomers,[20] the RT-NIL also turned out to be suitable for conjugated polymers.[21] In this letter, we apply RT-NIL on the conjugated light-emitting polymer (poly[2-methoxy-5-(2-ethylhexyloxy)-1,4-phenylenevinylene]) (MEH-PPV) to realize a polymeric DFB laser, exhibiting emission at 630 nm, with a full width at half maximum (FWHM) of 2.7 nm and a pump threshold of 25 μJ/cm^2. The RT-NIL technique allows us to obtain a high quality, reproducible pattern transfer, without reducing the polymer emission yield, which is strategic to realize organic-based optoelectronic devices.

The procedure for the preparation of the master by electron-beam lithography has been reported elsewhere.[20] The master (period, $\Lambda = 600$ nm) was directly exploited as a stamp for structuring a MEH-PPV film, spin cast at 2000 rpm for 40 s from $1.3 \times 10^{-5} M$ toluene solutions onto a quartz substrate. We obtained neat films of thickness of about 240 nm, measured by a profilometer. The imprinting process was carried out following the procedure described in Ref. 21, with an applied force of about 1.5 kN, corresponding to a pressure of 15 MPa applied onto the quartz substrates. We did not use any antisticking layer during the imprinting process. The cw-photoluminescence (PL) spectra of the imprinted film were obtained by pumping the samples with a He–Cd laser (325 nm). The DFB devices were then excited by the third harmonic (355 nm) of a 3 ns Q-switched neodymium doped yttrium aluminum garnet laser (repetition rate, 10 Hz). The pump beam was focused on a rectangular excitation stripe of width up to 500 μm and variable length (up to 1 cm), and the DFB emission was detected by a Si charge coupled device. In order to inhibit the photo-oxidation of MEH-PPV, the measurements were carried out in vacuum ambient (10^{-6} mbar).

The atomic force microscope topographic image of the imprinted MEH-PPV grating is displayed in Fig. 1. The sample exhibits a feature height of 42 ± 1 nm. Structures of higher aspect ratio can be obtained on MEH-PPV by increasing the imprinting time, thus allowing the polymer to fill a larger fraction of the stamp recessed features under pressure. Indeed, when the NIL is carried out at room temperature, the terminal-flow region of the polymer,[22,23] corresponding to an irreversible flow of amorphous material (i.e., to an irreversible deformation), is achieved by an imprinting time quite longer (one to two orders of magnitude) than that normally used for hot embossing. In particular, according to the

---

[a] Electronic mail: elisa.mele@unile.it

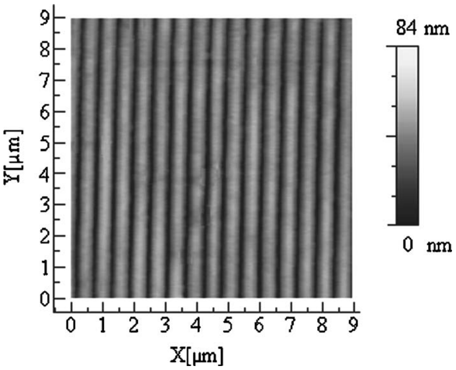

FIG. 1. Atomic force microscope two-dimensional topographic view of the 600 nm period patterned MEH-PPV grating.

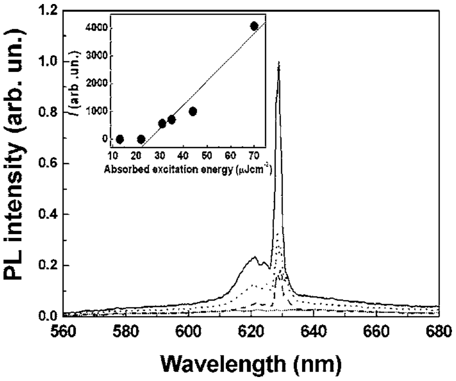

FIG. 3. DFB emission spectra collected under pulsed excitation (from bottom to top, the pump fluences are 22, 31, 44, and 70 μJ/cm^2). Inset: DFB peak emission intensity I vs absorbed excitation fluence. The solid line is a linear fit to the experimental data.

Adams-Gibbs model,[24] the structural relaxation time τ is related to the configurational entropy S_C by $\tau = \tau_0 \exp(C\Delta\mu / TS_C)$, where τ_0 and C are constants, and $\Delta\mu$ indicates the molecular energy barrier. The pressure dependence of S_C can be estimated by taking into account the molar thermal expansion of the amorphous system, $S_C(T,P) = \int_{T_K}^{T}[\Delta C_p(T')/T']dT' - \int_0^P \Delta(\partial V/\partial T)_{P'}dP'$, where T_K stands for the Kauzmann temperature and ΔC_p is the glass excess heat capacity.[25] Isothermally compressing the system results in (i) a volumetric contraction and (ii) a reduction of the configurational entropy and, consequently, determines a better stability of the imprinted pattern. Because of the irreversible deformation, the native specific volume per molecules can hardly be recovered even after removing the external stress. Indeed, gratings realized by RT-NIL could be stored for months under ambient conditions without observing losses in the achieved aspect ratio.

The effects of the superimposed periodic nanostructure on the PL properties of MEH-PPV were first analyzed by cw-PL measurements at different angles, collecting the light emitted in a small solid angle ($>10^{-3}$ rad) around each angle value, calculated by rotating the optical fiber in a plane perpendicular to the surface grating. The PL spectra of the printed DFB microcavity at 25°, 40°, and 45° are displayed in Fig. 2. The presence of a one-dimensional (1D) wavelength-scale periodic corrugation in the polymeric film determines an enhancement of the forward output from the active compound.[26,27] In particular, one emission peak is clearly visible in the PL spectra, with a strongly enhanced peak at 599 nm (at 45°), shifting to 619 nm (at 40°) and 704 nm (at 25°). In the DFB microcavities,[28] the emission angle Θ of the output wavelength λ is related to the period of the nanostructures Λ by the relation $(2\pi/\lambda)\sin\Theta = \pm(2\pi n_{\mathrm{eff}}/\lambda) \pm m2\pi/\Lambda$, where n_{eff} is the effective refractive index of the guided mode and m indicates the diffraction order inside the slab. The previous equation describes the conservation of the in-plane component of the wave vector of the output light $[k_0 = \pm(2\pi/\lambda)]$ and of the guided mode $[k_g = \pm(2n_{\mathrm{eff}}/\lambda)]$ by means of the Bragg vector (reciprocal lattice vector of the 1D photonic crystal structure, $G = 2\pi/\Lambda$).[28] The imprinted grating allows the light trapped in waveguide modes within the organic slab to be scattered out of the film along certain forward directions, thus reducing the self-absorption inside the organic layer. The dependence of the PL peak on the collection angle allows us to estimate the dependence of effective refractive index of the DFB structure on wavelength, decreasing from 1.73 to 1.57 upon increasing λ from 579 to 739 nm (inset of Fig. 2).

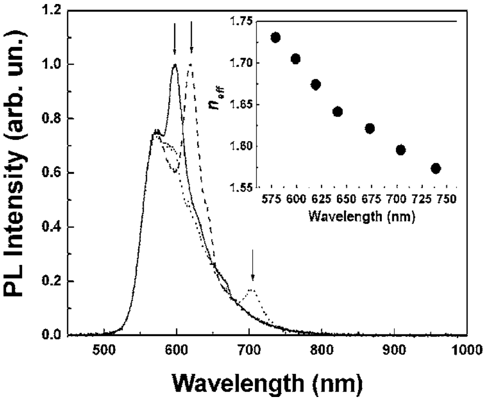

FIG. 2. cw-PL spectra from the active imprinted grating at $\Theta = 25°$ (dotted line), 40° (dashed line), and 45° (continuous line). The arrows indicate the peak shift upon increasing the detection angle. Inset: wavelength dependence of n_{eff}.

The PL spectra of our DFB lasers under pulsed excitation, as a function of the absorbed excitation fluence, are displayed in Fig. 3. At low excitation fluence (below 25 μJ/cm^2) the spectra are broad (FWHM $\sim$ 100 nm) and featureless, whereas, for higher pump energies, a narrow peak ($\lambda_m = 630$ nm, FWHM < 2.7 nm) arises within the gain spectral region of MEH-PPV (560–680 nm). According to the Bragg expression $m\lambda_m = 2n_{\mathrm{eff}}\Lambda$ and considering for the n_{eff} of MEH-PPV an average value of 1.6, the MEH-PPV DFB device works at the third order of diffraction, with both the refractive index and the optical gain modulated along the 1D periodic polymer/air interface. The threshold excitation fluence was measured to be 25 μJ/cm^2, and the laser emission intensity I above threshold exhibits a linear growth upon increasing the excitation fluence (inset of Fig. 3). Finally, we investigated the polarization properties of the imprinted DFB devices. We found that our lasers emit s-polarized light (with polarization parallel to the grating grooves, namely, corresponding to transversal electric guided modes). The spectra collected above the lasing threshold with s and p polarizations are displayed in Fig. 4. The polarization contrast, $\chi = (I_s - I_p)/(I_s + I_p)$, reaches values as high as 0.91, corresponding to a polarization ratio larger than 21 (inset of Fig. 4). This is comparable to the best values reported for DFB lasers based on tris(8-hydroxy quinoline) aluminium doped with

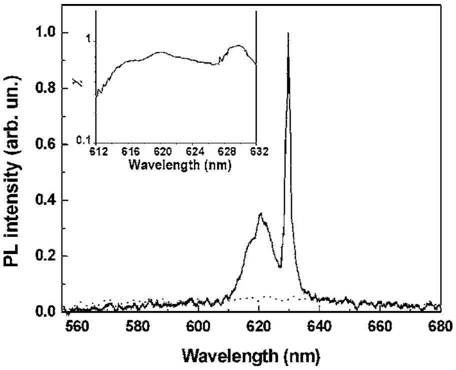

FIG. 4. Polarized PL spectra, parallel (continuous line) and perpendicular (dashed line) to the waveguide plane (excitation energy of 61 μJ/cm^2). Inset: spectral dependence of the polarization contrast (χ) in the gain region.

4-(dicyanomethylene)-2-methyl-6-(julolidin-4-yl-vinyl)-4*H*-pyran[29] and on spirobifluorene derivatives.[30]

In conclusion, we demonstrate that RT-NIL is remarkably convenient to fabricate high quality DBF lasers consisting of conjugated polymers. In particular, we realized a 1D grating with a period of 600 nm on MEH-PPV, providing laser emission at 630 nm with a lasing threshold of 25 μJ/cm^2 and a polarization contrast of 0.91. Moreover, we observed that the superimposed periodic corrugation induces an enhancement of the forward emitted light. RT-NIL is therefore strategic for producing stable patterns on light-emitting polymers for the fabrication of nanopatterned optoelectronic devices.

This work was partially supported by the Italian Minister of Education, University and Research through the PRIN Project No. 2005020804.

[1] R. H. Friend, R. W. Gymer, A. B. Holmes, J. H. Burroughes, R. N. Marks, C. Taliani, D. D. C. Bradley, D. A. Dos Santos, J. L. Brédas, M. Lögdlund, and W. R. Salaneck, Nature (London) **397**, 121 (1999).

[2] G. Yu, J. Wang, J. McElvain, and A. J. Heeger, Adv. Mater. (Weinheim, Ger.) **10**, 1431 (1998).

[3] K. M. Coakley and M. D. McGehee, Chem. Mater. **16**, 4533 (2004).

[4] C. D. Muller, A. Falcou, N. Reckefuss, M. Rojahn, V. Wiederhirn, P. Rudati, H. Frohne, O. Nuyken, H. Becker, and K. Meerholz, Nature (London) **421**, 829 (2003).

[5] H. Sirringhaus, N. Tessler, and R. H. Friend, Science **280**, 1741 (1998).

[6] M. D. McGehee and A. J. Heeger, Adv. Mater. (Weinheim, Ger.) **12**, 1655 (2000).

[7] N. Tessler, G. J. Denton, and R. H. Friend, Nature (London) **382**, 695 (1996).

[8] Y. Kawabe, C. Spiegelberg, A. Schulzgen, M. F. Nabor, B. Kippelen, E. A. Mash, P. M. Allemand, M. Kuwata-Gonokami, K. Takeda, and N. Peyghambarian, Appl. Phys. Lett. **72**, 141 (1998).

[9] S. V. Frolov, M. Shkunov, and Z. V. Vardeny, Phys. Rev. B **56**, R4363 (1997).

[10] H. Kogelnik and C. V. Shank, Appl. Phys. Lett. **18**, 152 (1971).

[11] M. D. McGehee, M. A. Diaz-Garcia, F. Hide, R. Gupta, E. K. Miller, D. Moses, and A. J. Heeger, Appl. Phys. Lett. **72**, 1536 (1998).

[12] N. Moll, R. F. Mahrt, C. Bauer, H. Giessen, B. Schnabel, E. B. Kley, and U. Scherf, Appl. Phys. Lett. **80**, 734 (2000).

[13] D. Pisignano, M. Anni, G. Gigli, R. Cingolani, G. Barbarella, L. Favaretto, and G. Sotgiu, Synth. Met. **137**, 1057 (2003).

[14] J. A. Rogers, M. Meier, A. Dodabalapur, E. J. Laskowski, and M. A. Cappuzzo, Appl. Phys. Lett. **74**, 3257 (1999).

[15] Y. Chou, P. R. Krauss, and P. J. Renstrom, Science **272**, 85 (1996).

[16] D. Pisignano, L. Persano, P. Visconti, R. Cingolani, G. Gigli, G. Barbarella, and L. Favaretto, Appl. Phys. Lett. **83**, 2545 (2003).

[17] M. Yan, L. J. Rothberg, F. Papadimitrakopoulos, M. E. Galvin, and T. M. Miller, Phys. Rev. Lett. **73**, 744 (1994).

[18] J. Wang, X. Sun, L. Chen, and S. Y. Chou, Appl. Phys. Lett. **75**, 2767 (1999).

[19] D.-Y. Khang, H. Yoon, and H. H. Lee, Adv. Mater. (Weinheim, Ger.) **13**, 749 (2001).

[20] D. Pisignano, L. Persano, M. F. Raganato, P. Visconti, R. Cingolani, G. Barbarella, L. Favaretto, and G. Gigli, Adv. Mater. (Weinheim, Ger.) **16**, 525 (2004).

[21] E. Mele, F. Di Benedetto, L. Persano, R. Cingolani, and D. Pisignano, Nano Lett. **5**, 1915 (2005).

[22] S. Zankovych, T. Hoffmann, J. Seekamp, J.-U. Bruch, and C. M. Sotomayor Torres, Nanotechnology **12**, 91 (2001).

[23] G. Strobl, *The Physics of Polymers* (Springer, Berlin, 1997), pp. 324–338.

[24] G. Adam and J. H. Gibbs, J. Chem. Phys. **43**, 139 (1965).

[25] R. Casalini, S. Capaccioli, M. Lucchesi, P. A. Rolla, and S. Corezzi, Phys. Rev. E **63**, 031207 (2001).

[26] B. J. Matterson, J. M. Lupton, A. F. Safonov, M. G. Salt, W. L. Barnes, and I. D. W. Samuel, Adv. Mater. (Weinheim, Ger.) **13**, 123 (2001).

[27] J. M. Ziebarth, A. K. Saafir, S. Fan, and M. D. McGehee, Adv. Funct. Mater. **14**, 451 (2004).

[28] G. A. Turnbull, P. Andrew, M. J. Jory, W. L. Barnes, and I. D. W. Samuel, Phys. Rev. B **64**, 125122 (2001).

[29] D. Schneider, S. Hartmann, T. Benstem, T. Dobbertin, D. Heithecker, D. Metzdorf, E. Becker, T. Riedl, H.-H. Johannes, W. Kowalsky, T. Weimann, J. Wang, and P. Hinze, Appl. Phys. B: Lasers Opt. **77**, 399 (2003).

[30] D. Schneider, T. Rabe, T. Riedl, T. Dobbertin, O. Werner, M. Kröger, E. Becker, H.-H. Johannes, W. Kowalsky, T. Weimann, J. Wang, P. Hinze, A. Gerhard, P. Stössel, and H. Vestweber, Appl. Phys. Lett. **84**, 4693 (2004).